The Astrophysical Journal, 749:76 (5pp), 2012 April 10 doi:10.1088/0004-637X/749/1/76

THE $v = 3 \leftarrow 0$ $S(0)$–$S(3)$ ELECTRIC QUADRUPOLE TRANSITIONS OF H_2 NEAR 0.8 μm

S.-M. Hu[1], H. Pan[1], C.-F. Cheng[1], Y. R. Sun[1], X.-F. Li[1], J. Wang[1], A. Campargue[2], and A.-W. Liu[1]
[1] Hefei National Laboratory for Physical Sciences at Microscale, University of Science and Technology of China, Hefei 230026, China; smhu@ustc.edu.cn, awliu@ustc.edu.cn
[2] Université Grenoble 1/CNRS, UMR5588 LIPhy Grenoble, F-38041, France
Received 2012 January 4; accepted 2012 February 6; published 2012 March 23

ABSTRACT

The very weak $S(0)$–$S(3)$ electric quadrupole transitions of the second overtone band of molecular hydrogen have been recorded in the laboratory by continuous-wave cavity ring-down spectroscopy near 0.8 μm. The ultrahigh sensitivity of the spectrometer ($\alpha_{min} \sim 1 \times 10^{-10}$ cm^{-1}) allows us to detect the considered transitions at a relatively low sample pressure (50–750 torr). The line positions, intensity, and pressure-shift coefficients are derived from a fit of the line shape using a Galatry profile. Compared with literature values, the relative differences between the experimental and theoretical transition intensities are reduced by one order of magnitude, reaching a value of about 2% mainly dependent of the line-shape function adopted for the profile fitting. The thermal equilibrium relative intensity of the $S(1)$ to $S(0)$ line is determined with an accuracy of 0.4%, which can be used to probe the *ortho*- to *para*-H_2 concentration ratio. Our measurements confirm the quality of the high-level ab initio calculations, including the relativistic and quantum electrodynamics corrections.

Key word: molecular data

Online-only material: color figures

1. INTRODUCTION

The hydrogen molecule is the most abundant molecule in the universe. The electric quadrupole transitions of H_2 are of particular interest to probe the atmosphere of planets, cold stars, and interstellar clouds. It was proposed by Herzberg (1938) that the extremely weak second overtone (3–0) transitions near 0.8 μm would be the most favorable in detecting molecular hydrogen in planetary or stellar spectra. The first laboratory measurement was carried out by himself (Herzberg 1949), which was also the first observation of the quadrupole transition in molecular spectra. The diffuse feature at 827 nm observed in the spectra of Uranus and Neptune was eventually assigned as the $S(0)$ line of the (3–0) band of H_2 (Herzberg 1952). This quadrupole band has also been utilized to identify the existence of H_2 in Jupiter's atmosphere (Kiess et al. 1960) and to retrieve the H_2 column density (Owen 1970).

In the last few decades, extensive laboratory studies have been carried out mainly using Fourier transform spectrometer integrated with long-absorption sample cells (Rank et al. 1966; Bragg et al. 1982). Because H_2 is the simplest neutral molecule, theoreticians have been able to obtain its energy levels and transition probabilities (Wolniewicz et al. 1998; Komasa et al. 2011) to very high accuracy using ab initio calculations. A recent review of these studies has been given by Campargue et al. (2012). In principle, overtone bands are more suitable to detect H_2, taking advantage of the enhanced sensitivity of detectors in the near-infrared and visible regions compared with the infrared region. But applications are limited by the uncertainties in the observed quadrupole transition probabilities. The measured (1–0) and (2–0) band transition intensities (Bragg et al. 1982) agree well with the calculated results (Wolniewicz et al. 1998; Campargue et al. 2012), but higher overtones (Bragg et al. 1982; Ferguson et al. 1993; Robie & Hodges 2006) show systematic deviations. In particular, a discrepancy up to 30% has been reported for the intensities of the (3–0) band transitions detected by a pulsed cavity ring-down (CRD) spectrometer (Robie & Hodges 2006). Due to the experimental uncertainty and the pressure shift, which has not been corrected, the line positions of the (3–0) band transitions given by Bragg et al. (1982) also show large discrepancies ($\sim 10^{-2}$ cm^{-1}) compared with the calculated results taking into account the relativistic and quantum electrodynamics (QED) corrections (Komasa et al. 2011).

This work is devoted to the laboratory spectroscopy study of the $S(J)$ ($J = 0$–3, $\Delta J = 2$) transitions of the ($v = 3 \leftarrow 0$) overtone using a sensitive CRD spectrometer with a sub-MHz precision. The purpose of this contribution is to derive accurate line parameters, including transition frequencies, intensities, and pressure-shift values, which can be used to verify the high-level theoretical calculations and be applied in astronomical studies.

2. EXPERIMENTAL

The $S(0)$–$S(3)$ lines of the (3–0) band of H_2 were measured between 796 and 828 nm at room temperature (296–298 K). Hydrogen gas samples (with a stated purity of 99.99%) with pressure values between 50 and 750 torr were used. The pressure was measured with a capacitance gauge (MKS 627B, 0.12% accuracy). The spectrum was recorded with a CRD spectrometer based on a continuous-wave Ti:Sapphire laser. The details of the experimental setup have been presented elsewhere (Gao et al. 2010; Pan et al. 2011) and only a brief description will be given here.

A beam from the tunable Ti:Sapphire laser (Coherent 899-21) is coupled to a 1.4 m long resonance cavity. The cavity mirrors (Los Gatos Inc.) have a reflectivity of 99.995% and one of the two mirrors is mounted on a piezoelectric actuator. The piezoelectric actuator is driven with a triangle wave from a function generator to match the cavity mode to the laser frequency. The Ti:Sapphire laser is running in a step-scan mode with a step size of 150 MHz. On each step, typically about 100 ring-down events are recorded with a fast digitizer. The digitizer is working at a sampling rate of 1 Mega samples per second with 14-bit resolution. A fitting program is applied to fit the exponential decay curve and to give the decay time τ. The

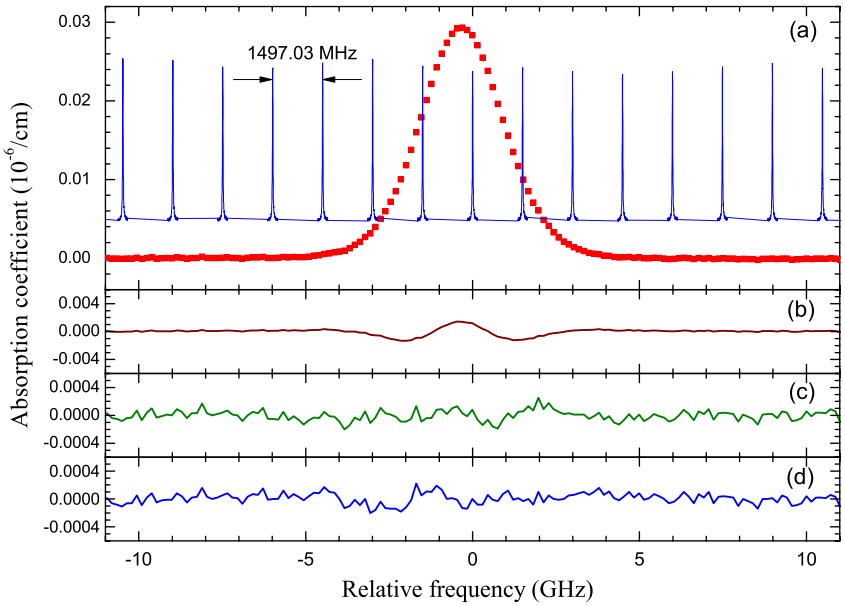

Figure 1. $S(1)$ line near 815 nm of H_2 recorded at 200 torr. (a) Observed CRDS spectrum together with the ULE-FPI transmission spectrum used for calibration. (b), (c), and (d) are the fitting residuals using Voigt, Rautian, and Galatry profiles, respectively. The Gaussian width was fixed at the Doppler width value in all the fittings.

(A color version of this figure is available in the online journal.)

sample-absorption coefficient, α, can be derived from

$$\alpha = \frac{1}{c}\left(\frac{1}{\tau} - \frac{1}{\tau_0}\right), \quad (1)$$

where c is the speed of light and τ and τ_0 are the decay time of the cavity with and without sample, respectively. The minimal detectable (noise-equivalent) absorption coefficient $\alpha_{\min}$ is 1×10^{-10} cm^{-1}. The ultrahigh sensitivity of the spectrometer allows the detection of very weak H_2 transitions with a sufficient signal-to-noise ratio at relatively low sample pressures. This has the advantage of limiting the impact of pressure-induced effects on the retrieved line parameters (Frommhold 1993).

A lambda-meter (Burleigh WA1500) with 0.002 cm^{-1} accuracy was used to monitor the *absolute* laser frequency during the measurements. To achieve a MHz *relative* frequency precision, the transmittance spectra of a thermo-stabilized Fabry-Pérot interferometer made of ultralow-expansion glass (ULE-FPI) were also recorded to calibrate the spectrum. The 10 cm long ULE-FPI is located in a vacuum chamber and the measured temperature drift is below 10 mK during the recordings (several days), which yields a frequency stability of the transmittance peaks estimated to be better than 1 MHz. The free spectral range was measured to be 1497.03(2) MHz in the region of 780–830 nm. The excellent stability of the ULE-FPI allows calibration of the CRD spectrum with a precision better than 1 MHz. For each studied transition, the CRDS spectrum was recorded on a 25 GHz spectral section around the H_2 line center. Figure 1(a) shows the $S(1)$ line near 815 nm together with the transmission spectrum of the ULE-FPI.

3. RESULTS AND DISCUSSION

The line profile of the hydrogen rovibrational transitions is well known to show a remarkable Dicke narrowing that increases with the pressure (Gupta et al. 2006; Robie & Hodges 2006; Kassi & Campargue 2011; Campargue et al. 2012). At pressure values over 90 torr, the speed dependence effect becomes significant compared with the Doppler and collision broadening effects (Lepère 2004). As a result of the collision effects, the profile cannot be reproduced by the conventional Voigt line shape (Figure 1(b)). Collision models from Galatry (1961) and Rautian & Sobelman (1967) take into account the effects of Doppler broadening, Dicke narrowing, and collision broadening. In this work, we adopt the "soft" collisional Galatry model, which was also applied in the study of the first overtone band of H_2 (Gupta et al. 2006; Campargue et al. 2012). The Gaussian width was fixed at the calculated Doppler width value, while other parameters, including the line position, intensity, Lorentzian width, and Dicke narrowing coefficients, were derived from the fitting. As illustrated in Figure 1, the $S(1)$ line profile recorded at 200 torr is reproduced within the experimental accuracy, and the residuals of the fit are at the experimental noise level.

The pressure shifts of the $S(0)$–$S(3)$ line centers are determined using the longitudinal modes of the ULE-FPI as frequency anchors. From a linear fit of the position values versus the pressures (Figure 2), the line position at the zero pressure limit together with the pressure shift coefficient are obtained (Table 1). The obtained line positions agree with the theoretically calculated values (Komasa et al. 2011) within their uncertainties (0.002 and 0.0025 cm^{-1}, respectively). The positions measured by Bragg et al. (1982) at 2.8 atm show a systematic difference on the order of -0.01 cm^{-1}, which is mostly due to the pressure shift. After correction, using the pressure-shift coefficients obtained here, the line centers of Bragg et al. (1982) agree with our values within the experimental uncertainty (see Table 1). To the best of our knowledge, the derived pressure-shift coefficients are the most accurate determinations for H_2 transitions. The pressure-shift coefficients of the (3–0) band have been predicted by Kelley & Bragg (1986), but their values are about 50% larger than ours.

The integrated-absorption coefficient values are also obtained from the fit of the spectra measured at various H_2 sample pressures. The resulting values converted to values at 296 K are plotted versus the pressure in Figure 3. A recent available partition function by Laraia et al. (2011) has been adopted in the

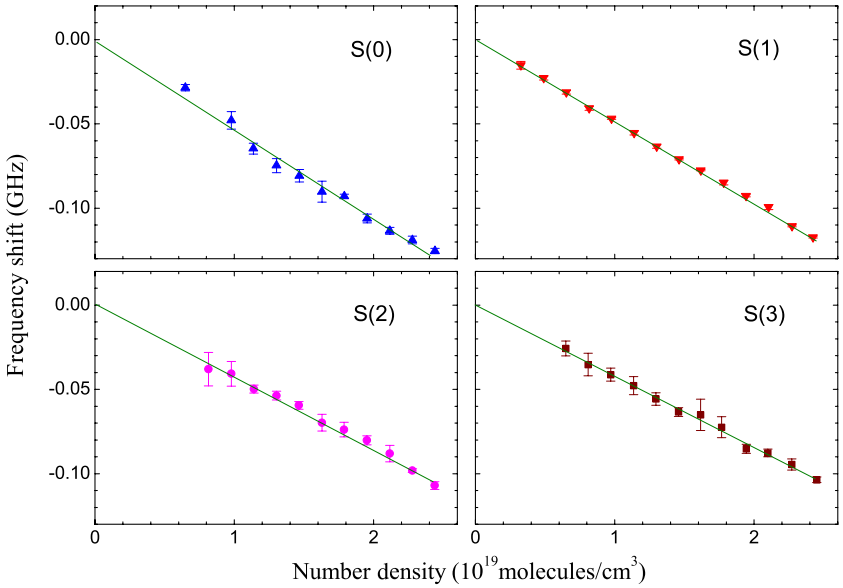

Figure 2. Pressure shifts of the $S(0)$–$S(3)$ lines of the (3–0) overtone of H_2.
(A color version of this figure is available in the online journal.)

Table 1
Line Parameters of the $S(J)$ (J = 0–3) Quadrupole Transitions of the (3–0) Band of H_2

Line	Line Position (cm^{-1})			γ^c	Intensity (296 K), (10^{-29} cm molecule^{-1})				A^f
	Calc.[a]	This Work	Bragg[b]		Calc.[a]	This Work[d]	Bragg[b]	Robie[e]	This Work[d]
$S(0)$	12084.6970(25)	.6963(20)	.6995(23)	−4.77(21)	12.77	12.52(3)	10.4(7)	9.3(11)	2.114(5)
$S(1)$	12265.5949(25)	.5929(20)	.5942(7)	−4.31(4)	49.40	49.11(2)	45 (3)	45.4(11)	3.618(1)
$S(2)$	12424.4421(25)	.4413(20)	.4444(37)	−3.80(13)	9.150	9.39(2)	9.3(7)	8.6(7)	5.213(11)
$S(3)$	12559.7492(25)	.7494(20)	.7522(59)	−3.77(9)	7.628	7.51(2)	6.7(11)	6.8(3)	6.404(17)

Notes.
[a] Calculated values taken from Komasa et al. (2011) and Campargue et al. (2012).
[b] From Bragg et al. (1982); position values corrected with the pressure-shift coefficients obtained in this work. Note that other digits in the observed positions are the same as those of the calculated values and then omitted.
[c] Pressure-shift coefficient, in 10^{-3} cm^{-1} $amagat^{-1}$, 1 amagat = 2.6867774×10^{19} molecule cm^{-3}.
[d] The deviations given here are only the statistical uncertainty. Other contributions are discussed in the text.
[e] From Robie & Hodges (2006).
[f] Einstein-A coefficient, in 10^{-8} s^{-1}.

conversion. The line intensities of the $S(J)$ ($J = 0$–3) transitions are derived from the linear fit included in the same figure. The derived values, together with the statistical deviations, are given in Table 1. The 1σ statistical standard deviation in line intensity is only about 0.2%. We estimate that the systematic uncertainty is 0.12% for the sample pressure and 0.3% for the temperature, which gives a combined systematic uncertainty of 0.4%. It is worth noting that, when different models are used in the spectral profile fitting, the retrieved line centers coincide, but there is a systematic deviation in the obtained line intensities. For illustration, the results obtained for $S(1)$ using the Rautian model are also shown in Figure 3. For the $S(1)$ line, the Galatry model leads to a line intensity, which is 2.4% larger than that obtained with the Rautian model. The main contribution to the uncertainty on our intensity values is then due to the choice of the profile function. Further investigation of the intermolecular collision mechanism is required to determine the most suitable profile and reduce the experimental uncertainty.

The comparison between the experimental and calculated line intensities (Wolniewicz et al. 1998; Campargue et al. 2012) are shown in Figure 4. There is a systematic deviation between the present results and that by Robie & Hodges (2006), which is about two to three times the standard deviation given by Robie & Hodges (2006) for $S(0)$, $S(1)$, and $S(3)$. The differences between our values and the calculated ones vary between −2% and +2%, which corresponds to the uncertainty related to the choice of the line profile function.

The Einstein-A coefficient A_{21} can be derived from the corresponding line intensity I using the equation given by Šimečková et al. (2006):

$$I(T) = \frac{g_2 \sigma_a}{Q_{\rm tot}(T)} \frac{A_{21}}{8\pi c \nu_0^2} \exp\left(-\frac{E_1}{k_B T}\right)\left[1 - \exp\left(-\frac{hc\nu_0}{k_B T}\right)\right], \quad (2)$$

where subscripts 1 and 2 denote the lower and upper energy levels, respectively. g_2 is the statistical weight of the level 2, σ_a is the isotopic abundance, $Q_{\rm tot}(T)$ is the total partition function at temperature T, which has been given by Laraia et al. (2011), ν_0 is the central transition frequency in cm^{-1}, E_1 is the energy of the level 1, and h, c, and k_B are the Planck constant, the speed of light, and the Boltzmann constant, respectively. The obtained values of Einstein-A coefficients are included in Table 1. The

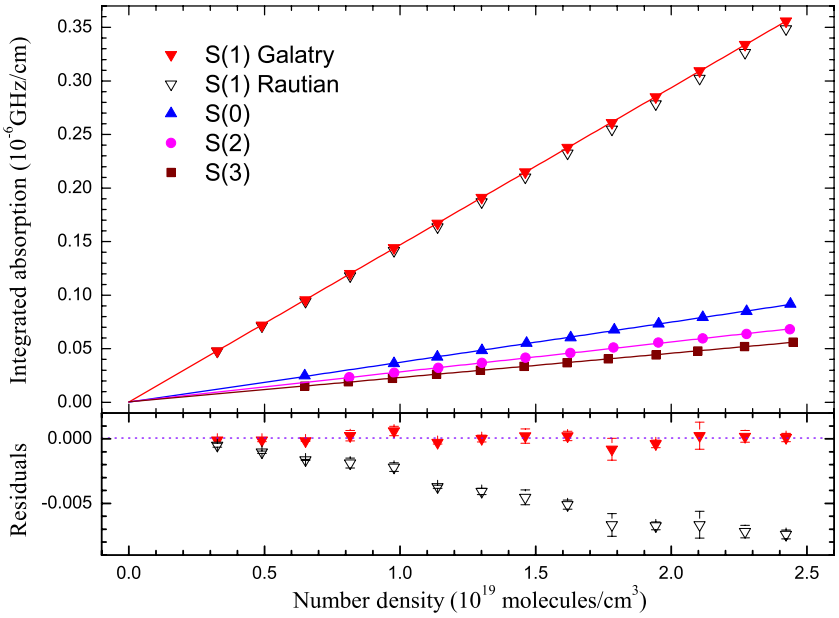

Figure 3. Experimental integrated-absorption coefficient of transitions observed with different H_2 molecular density. The Galatry profile fitting was adopted for $S(0)$–$S(3)$. For comparison, Rautian profile fitting (open triangle) was also applied for $S(1)$. The residuals of the linear fit of $S(1)$ are given in the lower panel for the Galatry and Rautian fits.

(A color version of this figure is available in the online journal.)

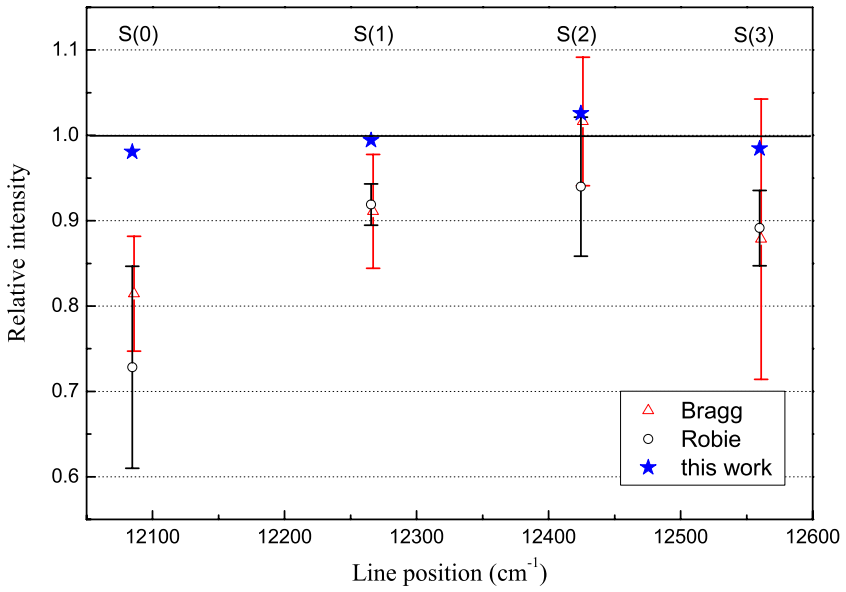

Figure 4. Comparison of the experimental and calculated line intensities ($I_{obs.}/I_{calc.}$ at 296 K) of $S(0)$–$S(3)$. Calculated line intensities are taken from Campargue et al. (2012). The triangles, circles, and stars represent values given by Bragg et al. (1982), Robie & Hodges (2006), and this work, respectively.

(A color version of this figure is available in the online journal.)

entire set of the calculated values has been provided in the database attached to Campargue et al. (2012).

The transitions observed here can be used to determine the molecular hydrogen column density and the temperature of the target sample. Note that, in Equation (2), the *ortho*- to *para*-H_2 ratio $\gamma(T) = [ortho\text{-}H_2]/[para\text{-}H_2]$ is assumed to be at thermal equilibrium at temperature T. The equilibrium *ortho*- to *para*-H_2 ratio γ^e is about 3:1 at room temperature, 1:1 at 77 K, and almost 0 at 20 K. But, in the absence of catalyst, it takes an extremely long time to reach equilibrium. Nonequilibrium *ortho*- to *para*-H_2 ratios have been observed in the interstellar medium by Neufeld et al. (1998), Fuente et al. (1999), and Neufeld et al. (2006). For the H_2 gas sample with a nonequilibrium *ortho*- to *para*-H_2 ratio, the partial concentration of *ortho* (*para*) H_2 in the sample, σ_o (σ_p), should be included in the line intensity formula of an *ortho* (*para*) H_2 transition at a given temperature T:

$$I_o(T) = \sigma_o \frac{I_o^e(T)}{\sigma_o^e(T)} \tag{3}$$

$$I_p(T) = \sigma_p \frac{I_p^e(T)}{\sigma_p^e(T)}, \tag{4}$$

where $\sigma_p + \sigma_o = 1$, $\gamma = \sigma_o/\sigma_p$, and the superscript e denotes the corresponding values at thermal equilibrium. The temperature

T can be derived from the relative intensity of two transitions of either *para*-H_2 or *ortho*-H_2 using Equation (2).

Since the thermal equilibrium *ortho*-to-*para* ratio γ^e can be accurately calculated at a given temperature, any nonequilibrium *ortho*-to-*para* ratio γ can be determined by measuring the relative intensity of the $S(0)$ and $S(1)$ lines, $I_{S(1)}/I_{S(0)}$:

$$\frac{1}{\gamma}\cdot\frac{I_{S(1)}}{I_{S(0)}}=\frac{1}{\gamma^e(T)}\cdot\frac{I^e_{S(1)}(T)}{I^e_{S(0)}(T)}. \quad (5)$$

The equilibrium relative intensity $I^e_{S(1)}/I^e_{S(0)}$ determined in this work is 3.923 at 296 K. Since the systematic deviation induced by the line profile is identical for the $S(0)$ and $S(1)$ lines, the uncertainty of the obtained $I_{S(0)}/I_{S(1)}$ value is mainly due to the statistical uncertainty and from the uncertainty in temperature measurements, which gives a combined uncertainty of about 0.4%. As a comparison, the calculated value is 1.4% smaller (3.868), while the values given by Bragg et al. (1982) and by Robie & Hodges (2006) are 10% and 20% larger, respectively.

4. SUMMARY AND CONCLUSIONS

The $S(0)$, $S(1)$, $S(2)$, and $S(3)$ electric quadrupole transitions of the ($v = 3 \leftarrow 0$) overtone band of molecular hydrogen in the electronic ground state have been recorded using a very sensitive continuous-wave CRD spectroscopy. With a minimal detectable absorption coefficient $\alpha_{\min} \sim 1 \times 10^{-10}$ cm^{-1} and a frequency precision of 1 MHz, the line positions, intensities, and pressure-shift coefficients were determined. Dicke narrowing of the line profiles has been observed, and the line parameters were derived from a fit of the line shape using a Galatry profile. After correcting the pressure shift, the obtained line positions agree well with the high-level ab initio calculations, including the relativistic and QED corrections. The discrepancy is below the experimental and theoretical uncertainties. The obtained pressure-shift coefficients are the most accurate for the H_2 quadrupole transitions reported so far, showing that the previous predicted values are about 50% overestimated. The intensities and Einstein-A coefficients of the transitions are obtained with an uncertainty of about 2%. The accuracy can be potentially improved if the mechanism of the collision can be better understood, resulting in a more reliable line shape function that could be used in the line profile fitting. The experimental values of the line intensities are found to be in very good agreement with the theoretical values (deviations less than 2%). The relative line intensities reported here with an estimated uncertainty of 0.4% can be used to obtain the temperature of the H_2 cloud and to probe the nonequilibrium *ortho*- to *para*-H_2 ratio.

This work is jointly supported by NSFC (90921006, 20903085, and 20873132), NKBRSF (2007CB815203 and 2010CB923300), and FRFCU. The support of the Groupement de Recherche International SAMIA between CNRS (France) and CAS (China) is also acknowledged.

REFERENCES

Bragg, S. L., Brault, J. W., & Smith, W. H. 1982, ApJ, 263, 999
Campargue, A., Kassi, S., Pachucki, K., & Komasa, J. 2012, Phys. Chem. Chem. Phys., 14, 802
Ferguson, D. W., Rao, K. N., Mickelson, M. E., & Larson, L. E. 1993, J. Mol. Spectorsc., 160, 315
Frommhold, L. 1993, Collision-induced Absorption in Gases (Cambridge: Cambridge Univ. Press)
Fuente, A., Martin-Pintado, J., Rodriguez-Fernandez, N. J., et al. 1999, ApJ, 518, L45
Galatry, L. 1961, Phys. Rev., 122, 1218
Gao, B., Jiang, W., Liu, A.-W., et al. 2010, Rev. Sci. Instrum., 81, 043105
Gupta, M., Owano, T., Baer, D. S., & O'Keefe, A. 2006, Chem. Phys. Lett., 418, 11
Herzberg, G. 1938, ApJ, 87, 428
Herzberg, G. 1949, Nature, 163, 170
Herzberg, G. 1952, ApJ, 115, 337
Kassi, S., & Campargue, A. 2011, J. Mol. Spectorsc., 267, 36
Kelley, J. D., & Bragg, S. L. 1986, Phys. Rev. A, 34, 3003
Kiess, C. C., Corliss, C. H., & Kiess, H. K. 1960, ApJ, 132, 221
Komasa, J., Piszczatowski, K., Yach, G., et al. 2011, J. Chem. Theory Comput., 7, 3105
Laraia, A. L., Gamache, R. R., Lamouroux, J., Gordon, I. E., & Rothman, L. S. 2011, Icarus, 215, 391
Lepère, M. 2004, Spectrochim. Acta A, 60, 3249
Neufeld, D. A., Melnick, G. J., & Harwit, M. 1998, ApJ, 506, L75
Neufeld, D. A., Melnick, G. J., Sonnentrucker, P., et al. 2006, ApJ, 649, 816
Owen, T. 1970, Science, 167, 1675
Pan, H., Cheng, C.-F., Sun, Y. R., et al. 2011, Rev. Sci. Instrum., 82, 103110
Rank, D. H., Fink, U., & Wiggins, T. A. 1966, ApJ, 143, 980
Rautian, S. G., & Sobelman, I. 1967, Sov. Phys. Uspekhi-Ussr, 9, 701
Robie, D., & Hodges, J. 2006, J. Chem. Phys., 124, 024307
Šimečková, M., Jacquemart, D., Rothman, L. S., Gamache, R. R., & Goldman, A. 2006, J. Quant. Spectrosc. Radiat. Transfer, 98, 130
Wolniewicz, L., Simbotin, I., & Dalgarno, A. 1998, ApJS, 115, 293